Supplemental Experimental Procedures

Sample preparation for mass spectrometry. Phosphorylated CTD affinity purified samples in 2% (v/v) Sarkosyl were precipitated with the addition of 10% (w/v) porcine insulin (Sigma), 0.1% (w/v) sodium deoxycholate, and 20% (w/v) trichloroacetic acid at 4ºC. Precipitated protein was pelleted and washed two times with -20ºC acetone and air dried. Samples were prepared for mass spectrometry using a modified version of the filter-aided sample prep (FASP) method (Wisniewski et al., 2009). Samples were solubilized in 4%(w/v) sodium dodecyl sulfate (SDS), 100mM Tris pH 8.5, 10mM TCEP, boiled and allowed to reduce for 20 min, followed by alkylation with 25mM iodoacetamide for 30 min in the dark. The reduced and alkylated proteins were then transferred to a 30kD MWCO Amicon Ultra (Millipore) ultrafiltration device and concentrated, washed three times with 8M urea, 100mM Tris pH 8.5, and again three times with 2M urea, 100mM Tris pH 8.5. One microgram endoprotease LysC (Wako) was added and incubated for 3h rocking at ambient temperature, followed by one microgram trypsin (Promega), rocking overnight at ambient temperature. Tryptic peptides were collected by centrifugation and desalted using C-18 spin columns (Pierce, ThermoScientific) and stored dry at -80ºC.

Purification of GST-fusions of the mammalian pol II C-terminal domain (CTD). The 52 repeat full-length CTD from mouse RNA polymerase II subunit Rpb1, along with the first 26 repeats of the promixal CTD and the last distal 26 repeats (repeats 27-52), each including the C-terminal sequence, were expressed from a pGEX vector (GE lifesciences) in RIPL Codon Plus BL21 DE3 cells (Agilent). GST-CTD fusion proteins were lysed with B-PER (Thermo Scientific) with protease inhibitors (0.25mM PMSF, 1mM Sodium metabisulfite, 1mM Benzamidine, 1mM DTT, and aprotinin) and cleared, then captured with GSH-Sepharose 4B (GE lifescience). GSH-Sepharose resin was washed with 500 column volumes 50 mMTris pH7.9, 8mM CHAPS, 1M NaCl, 0.5mM EDTA, 10% (v/v) glycerol, 0.5% (v/v) NP-40, then 200 column volumes 20mM HEPES, 0.1mM EDTA, 10% (v/v) Glycerol, 0.1% (v/v) NP-40, 500mM KCl, then 100 column volumes with the same buffer, only 150mM KCl. Beads were sampled using PAGE/Coomassie staining to verify yield and purity. Crudely purified GST-CTD was eluted from GSH-Sepharose resin with three rounds of two column volumes 30mM GSH in 80mM Tris pH 7.9, 0.1mM EDTA, 10%(v/v) glycerol, 0.02% (v/v) NP-40, 150mM KCl, then filtered with a 0.2um PVDF (Millipore) and concentrated in a 30kD MWCO Amicon Ultra (Millipore) to a final volume of approximately 100 µL, and sampled with PAGE/Coomassie. The entire sample was then loaded onto a Superdex 200 size exclusion column (running at 0.25mL/min) equilibrated in 25mM Tris pH 7.9, 150mM KCl, 0.1mM EDTA, 10%(v/v) glycerol. Thirty 250 µL fractions were collected and analyzed via PAGE/Coomassie.

Preparation of HeLa nuclear extract and nuclear pellet. HeLa nuclear extract was prepared from isolated nuclei as described (Dignam et al., 1983). The insoluble pellet from the nuclear extract (i.e. the nuclear pellet) was solubilized with 100mM HEPES pH7.9, 2mM $MgCl_2$, 100mM KCl, 20% (v/v) glycerol, protease inhibitors (0.25mM PMSF, 1mM Sodium metabisulfite, 1mM Benzamidine, 1mM DTT, and aprotinin), phosphatase inhibitors (1uM Microcystin LR (Enzo lifesciences), 0.1mM Sodium orthovanadate, 10mM beta-glycerophosphate, 5mM sodium fluoride, 1mM sodium pyrophosphate (all Sigma)), and nucleases Benzonase, RNAse A, and DNAse I. The pellet with chopped and dounced 20 times, and mixed overnight with a stirbar at 4ºC. The extract was cleared and aliquoted for storage at -80ºC.

Purification of human TFIIH. Approximately two grams of HeLa nuclear extract total protein was loaded onto a P11 phosphocellulose (Whatman) column equilibrated with 20mM HEPES, pH 7.4, 0.1mM EDTA, 10% Glycerol, 0.1% NP-40 and 0.1M KCl and washed to baseline. Step elutions of 0.3M, 0.5M and 1M KCl were collected and dialyzed to 0.1M KCl. The P11 1M KCl fraction was loaded onto a POROS Q (Applied Biosystems) column and washed to baseline with 0.1M KCl. Step elutions of 0.4M and 1M KCl were collected and dialyzed to 0.1M KCl. The Q0.4M KCl fraction was loaded on an anti-ERCC3 affinity column, washed with 1M KCl, then with 0.2M KCl prior to four peptide elutions (1 column volume each). Kinase activity of the purified TFIIH was measured using a highly purified GST-fusion of the C-terminal domain (CTD) of the mammalian RNA Polymerase II, as described (Knuesel et al., 2009b). An overview of the TFIIH purification is shown in **Figure S1A**.

Purification of human Positive Transcription Elongation Factor b (P-TEFb). This purification was adapted from (Tahirov et al., 2010). Sf9 cells were co-infected with plasmids expressing CDK9 (residues 1-345) and CCNT1. Approximately 1.25 liters of Sf9 cell pellet was lysed in 7mL B-PER II (78260 ThermoScientific), 5mM Imidazole, 150mM NaCl, 1% (v/v) Triton X-100, 2mM $MgCl_2$, 70U DNase I, and protease inhibitors (0.25mM PMSF, 1mM Sodium metabisulfite, 1mM Benzamidine, 1mM DTT, and aprotinin). The lysate was then dounced 25 times on ice and the NaCl concentration was brought up to 0.5M, then centrifuged at 100,000 x g for 60 minutes at 4ºC. This was added to 1.5mL washed Ni-NTA-agarose (Qiagen) and mixed for 60 minutes at 4ºC. The bound resin was pelleted at 150 x g and washed with 16 column volumes 20mM Tris pH 7.9, 5mM imidazole, 500mM NaCl, 1% (v/v) Triton X-100 and protease inhibitors in a gravity flow column. Next, the column was washed with 10 column volumes 20mM Tris pH 7.9, 25mM imidazole, 1M NaCl, 1%(v/v) Triton X-100 and protease inhibitors, then 10 column volumes 25mM Tris pH 7.9, 25mM imidazole, 70mM KCl, 15% (v/v) glycerol, 0.1mM EDTA, 1%(v/v) Triton X-100 and protease inhibitors. P-TEFb was eluted from the resin with 4 column volumes 25mM Tris pH 7.9. 500mM imidazole, 70mM KCl, 15%(v/v) glycerol, 0.1mM EDTA, 1%(v/v) Triton X-100 and protease inhibitors. The imidazole elution was diluted 6x with Mono S buffer A, 25mM HEPES pH 7.9, 150mM KCl, 15% (v/v) glycerol with 1mM DTT and 0.25mM PMSF, loaded onto a Mono S column (GE lifesciences), and washed to baseline. P-TEFb was eluted with a gradient to 1M KCl in 20 column volumes, while 50 µL fractions were collected. Fractions were screened by PAGE separation and either coomassie or silver staining and western blotting for CDK9 and CCNT1. Kinase activity of the purified P-TEFb was measured using a highly purified GST-fusion of the pol II CTD, as described (Knuesel et al., 2009b). An overview of the P-TEFb purification is shown in **Figure S1D**.

Generation of TFIIH- and P-TEFb-phosphorylated pol II CTD for pulldowns. Highly purified GST-CTD fusions were quantified using PAGE/Coomassie staining against a known amount of a standard protein. Kinase reactions using highly purified TFIIH and P-TEFb were performed with 50pmol of either GST-full length CTD (repeats 1-52), proximal CTD (repeats 1-26), or distal CTD (repeats 27-52). Buffer only was added for the mock kinase control to generate the unphosporylated CTD for pulldowns. GST-CTD kinase substrates were added to the kinase buffer containing 15mM Tris pH 7.9, 10mM $MgCl_2$, 50mM KCl, 2mM DTT, either kinase TFIIH or P-TEFb were added, and finally 500 μM ATP was added. Reactions were incubated at 30ºC and sampled over two hours by PAGE/Silver staining. Kinase reactions were diluted into 20mM HEPES, 0.1mM EDTA, 15%(v/v) glycerol, 150mM KCl, protease inhibitors and phosphatase inhibitors, 1 μM Microcystin LR (Enzo lifesciences), 0.1mM Sodium orthovanadate, 10mM beta-glycerophosphate, 5mM sodium fluoride, 1mM sodium pyrophosphate (all Sigma). (All buffers contained both protease and phosphatase inhibitors from here out.) Diluted kinase reactions were added to GSH-Sepharose resin to capture the phosphorylated/unphosphorylated GST-CTD, and resin was washed with 20 column volumes 20mM HEPES, 0.1mM EDTA, 10% (v/v) glycerol, 0.02% NP-40, 150mM KCl, with protease and phosphatase inhibitors. All the buffer was removed from the un/phosphorylated GST-CTD affinity resin, and approximately 5mg HeLa nuclear extract, supplemented with Benzonase, was added and mixed at 4ºC overnight. The GST-CTD affinity resin was washed with 75 column volumes 500mM KCl, 20mM HEPES, 0.1mM EDTA, 10%(v/v) glycerol, 0.1% (v/v) NP-40 and then with 50 column volumes 150mM KCl, 20mM HEPES, 0.1mM EDTA, 10%(v/v) glycerol, 0.02% (v/v) NP-40 with protease and phosphatase inhibitors. All buffer was then removed from the resin. To elute the protein-protein interactors, while leaving the excess GST-CTD affinity ligand immobilized to the resin, one column volume 2%(v/v) Sarkosyl in 0.15M HEGN without PIs/PhIs was added, removed and repeated, then combined, and sampled for PAGE/Silver staining. Finally, 8M urea was added to the resin to release the GST-CTD affinity ligands for PAGE/Silver staining comparative analysis of before and after to confirm the affinity ligand was not degraded throughout the experiment.

Cell lines. Wild-type (WT) and isogenic homozygous CDK7 analog-sensitive (CDK7as) HCT116 cells were provided by R. Fisher (Mt. Sinai School of Medicine) and validated by STR analysis. The cells were maintained in McCoys media supplemented with 10% FBS and penicillin/streptomycin. All experiments were performed after treating both WT or CDK7as cells for 24hr with 10μM NM-PP1 inhibitor (Toronto Research Chemicals), diluted from a 20mM stock in DMSO. THZ1 (Calbiochem) was used at 1μM, diluted from a 1mM stock in DMSO, for 1 hour treatment.

ChIP-Seq antibodies. Rabbit anti-pol II CTD (Schroeder et al., 2000), anti-histone H3 C-terminus and H3K4me3 (Zhang et al., 2005), H3K36me3 (Kim et al., 2011) and capping enzyme (Glover-Cutter et al., 2008) have been described. Rat monoclonal anti-Ser2-P (3E10) and Ser5-P (3E8) (Chapman et al., 2007; Mayer et al., 2012) were from Chromotek and gifts of D. Eick and were used with rabbit anti-Rat IgG (10mg/IP Jackson ImmunoResearch).

Methyltransferase assays. About 500ng of purified GST-CTD was incubated with 10 μL purified TFIIH for five hours in kinase buffer (25 mM Tris pH 7.9, 50 mM KCl, 10 mM $MgCl_2$, 2 mM DTT, 1 mM Benzamidine, 1 mM Sodium Metabisulfite, 1 μM Microcystin LR and 300 μM ATP) at 37°C in a final volume of 20 μL. This ensured a single, hyper-phosphorylated CTD, based upon silver stain analysis. Control reactions containing either GST-CTD or TFIIH only were incubated alongside. Aliquots of the kinase reactions were taken at the beginning and end of the incubation, separated by polyacrylamide gel electrophoresis and silver stained to insure full phosphorylation of the CTD. The kinase reactions were then placed on ice while assembling the SETD1A/B methyltransferase reactions.

For the methyltransferase assays, we used a buffer system based upon our *in vitro* transcription assays on chromatin templates (Knuesel et al., 2009a). A nucleosome master mix was first made containing 0.25 mg/mL non-linker ended trinucleosomes (NLE-Tri), 62.5 μg/mL S-Adenosyl Methionine, 0.6 mM Benzamidine, 0.6 mM Sodium Metabisulfite, 0.6 mM Phenyl Methyl Sulfonyl Fluoride, about 1 μg/mL Aprotinin, 1.6 μM Microcystin LR, 1.6 mM DTT and 1.6X Chromatin Assembly Buffer (5X stock contains 50 mM HEPES pH 7.6, 300 mM KCl, 35% glycerol, 30 mM $MgCl_2$, 0.5 mM EDTA, 0.5 mM EGTA, 2.5% Polyvinyl alcohol 9-10 KDa and 2.5% Polyethylene glycol 20 KDa). NLE-Tri were prepared as described (Muthurajan et al., 2014). The mix was then aliquoted into 8 μL and 1.5 μL of the appropriate kinase reaction was added. Then, either 3 μL FLAG-purified SETD1A or SETD1B was added. The reactions were incubated at 30°C for either 3 or 16 hours. Reactions were stopped by adding 12.5 μL of 2X Laemmli loading buffer and flash freezing in liquid nitrogen.

For westerns to detect the different H3K4 methylation marks, each reaction was divided four times and separated on a 15% denaturing PAGE gel. The proteins were then transferred to a 0.2 μm PVDF membrane and blocked for 1 hour in 5% milk in TBS-T. The blots were then rocked at 4°C overnight in TBS-T and primary antibodies against H3 total, H3K4me1, H3K4me2 or H3K4me3. The next morning, the blots were washed thoroughly in TBS-T and incubated with the secondary antibody for 1 hour in 5% milk in TBS-T. The blots were then washed in TBS-T and visualized on an ImageQuant LAS4000.

Purification of SETD1A and SETD1B complexes. Flag-SETD1A and -SETD1B HEK293 stable cell lines were cultured in DMEM with 10% FBS in the presence of 50μg/ml Hygromycin (Sigma). Doxycycline (final 2 μg/ml) was used to induce Flag-SETD1A and SETD1B expression for 48 hours. For complex purification, 3-4 ml HEK293 cell pellets were used for nuclear extract preparation and Flag affinity purifications were performed with M2 anti-Flag–agarose (Sigma) in the presence of Benzonase (Sigma). The M2 beads were washed with wash buffer (10mM HEPES (pH 7.9), 1.5mM $MgCl_2$, 300mM NaCl, 10mM KCl, 0.2% TritonX-100, w/ Protease inhibitor cocktail (Sigma P8340, add 1/500~1/1000 vol.)) four times. The complexes were eluted with 3x100 μl elution buffer (10mM HEPES (pH7.9), 0.1M NaCl, 1.5mM $MgCl_2$, 0.05% Triton X-100 w/ protease inhibitor cocktail (Sigma P8340) and 10% glycerol) containing 3XFlag peptide.

Western blot antibodies. Total Pol II: Santa Cruz, sc-899, N-terminus of RPB1, Lot # D2607; phospho-Ser5: Millipore, 3E8, Ser5 phosphorylation of the CTD of RPB1, Lot # 2585825; phospho-Ser2: Millipore, 3E10, Ser2 phosphorylation of the CTD of RPB1, Lot # 2276409; phospho-Ser7: Millipore, 4E12, Ser7 phosphorylation of the CTD of RPB1, Lot # 1951949; CDK7: Santa Cruz, sc-856, residues 1-346, Lot # C1914; p89/XPB: Santa Cruz, sc-293, C-terminus of TFIIH subunit p89, Lot # C0708; TBP: Santa Cruz, sc-273, Residues 1-300, Lot # A1811; H3K36me3: Abcam, ab9050, human histone H3 aa 1-100 (trimethyl K36); SETD1A, Total H3, and H3K4me1, H3K4me2, H3K4me3 were rabbit polyclonal lab stocks from A. Shilatifard.

Supplemental References

Chapman, R.D., Heidemann, M., Albert, T.K., Mailhammer, R., Flatley, A., Meisterernst, M., Kremmer, E., and Eick, D. (2007). Transcribing RNA polymerase II is phosphorylated at CTD residue serine-7. Science *318*, 1780-1782.

Dignam, J.D., Martin, P.L., Shastry, B.S., and Roeder, R.G. (1983). Eukaryotic gene transcription with purified components. Methods Enzymol *101*, 582-598.

Glover-Cutter, K., Kim, S., Espinosa, J.M., and Bentley, D.L. (2008). RNA polymerase II pauses and associates with pre-mRNA processing factors at both ends of genes. Nat Struct Mol Biol *15*, 71-78.

Kim, S., Kim, H., Fong, N., Erickson, B., and Bentley, D.L. (2011). Pre-mRNA splicing is a determinant of histone H3K36 methylation. Proc Natl Acad Sci U S A *108*, 13564-13569.

Knuesel, M.T., Meyer, K.D., Bernecky, C., and Taatjes, D.J. (2009a). The human CDK8 subcomplex is a molecular switch that controls Mediator co-activator function. Genes Dev *23*, 439-451.

Knuesel, M.T., Meyer, K.D., Donner, A.J., Espinosa, J.M., and Taatjes, D.J. (2009b). The human CDK8 subcomplex is a histone kinase that requires Med12 for activity and can function independently of Mediator. Mol Cell Biol *29*, 650-661.

Loven, J., Hoke, H.A., Lin, C.Y., Lau, A., Orlando, D.A., Vakoc, C.R., Bradner, J.E., Lee, T.I., and Young, R.A. (2013). Selective inhibition of tumor oncogenes by disruption of super-enhancers. Cell *153*, 320-334.

Mayer, A., Heidemann, M., Lidschreiber, M., Schreieck, A., Sun, M., Hintermair, C., Kremmer, E., Eick, D., and Cramer, P. (2012). CTD tyrosine phosphorylation impairs termination factor recruitment to RNA polymerase II. Science *336*, 1723-1725.

Muthurajan, U.M., Hepler, M.R., Hieb, A.R., Clark, N.J., Kramer, M., Yao, T., and Luger, K. (2014). Automodification switches PARP-1 function from chromatin architectural protein to histone chaperone. Proc Natl Acad Sci U S A *111*, 12752-12757.

Schroeder, S.C., Schwer, B., Shuman, S., and Bentley, D. (2000). Dynamic association of capping enzymes with transcribing RNA polymerase II. Genes Dev *14*, 2435-2440.

Schwanhausser, B., Busse, D., Li, N., Dittmar, G., Schuchhardt, J., Wolf, J., Chen, W., and Selbach, M. (2011). Global quantification of mammalian gene expression control. Nature *473*, 337-342.

Tahirov, T.H., Babayeva, N.D., Varzavand, K., Cooper, J.J., Sedore, S.C., and Price, D.H. (2010). Crystal structure of HIV-1 Tat complexed with human P-TEFb. Nature *465*, 747-751.

Wisniewski, J.R., Zougman, A., Nagaraj, N., and Mann, M. (2009). Universal sample preparation method for proteome analysis. Nat Methods *6*, 359-362.

Zhang, L., Schroeder, S., Fong, N., and Bentley, D.L. (2005). Altered nucleosome occupancy and histone H3K4 methylation in response to 'transcriptional stress'. EMBO J *24*, 2379-2390.

Figure S1

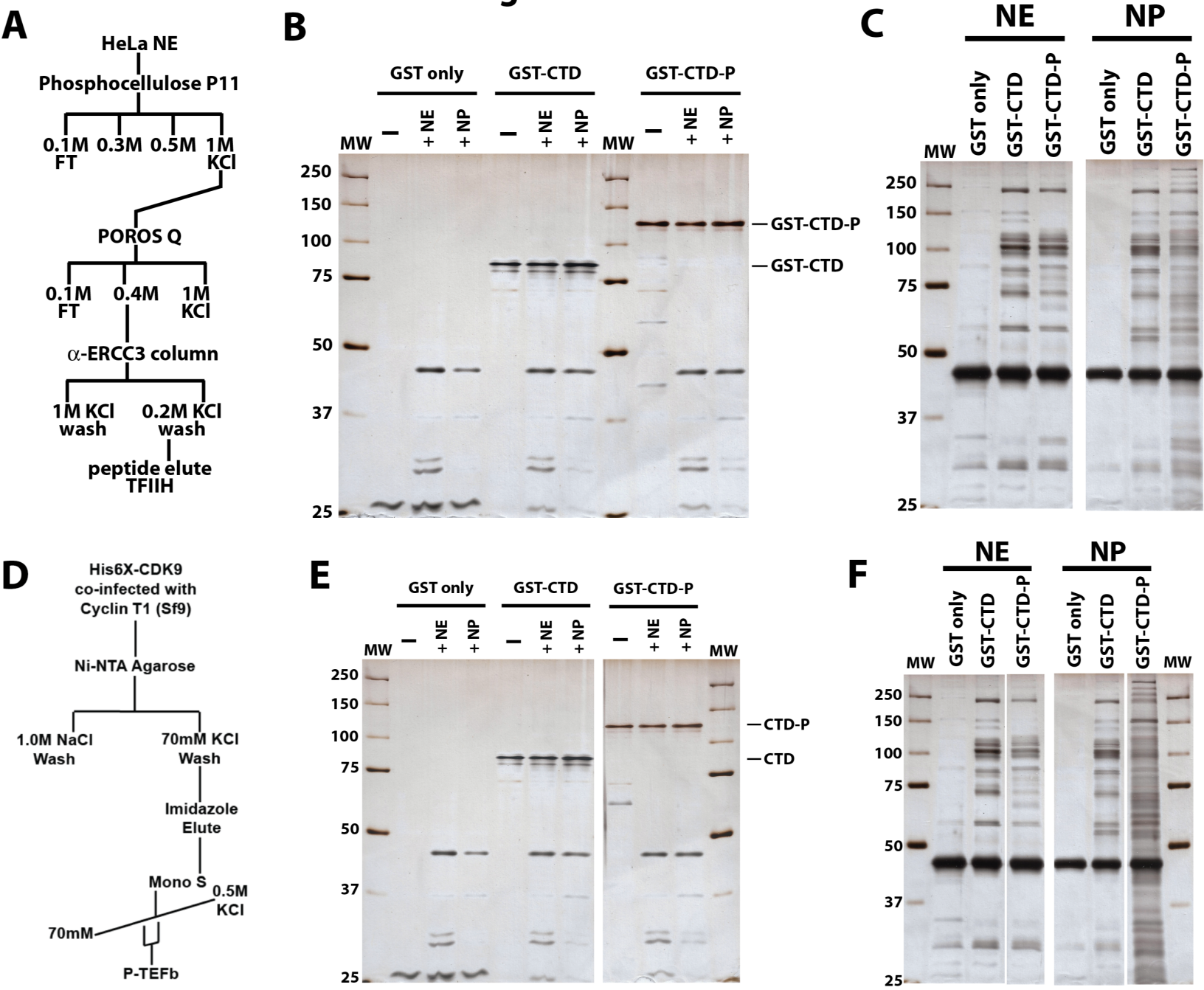

Figure S1 (related to Figure 1, 2, 6). CTD phosphorylation is maintained during incubation with HeLa nuclear extract (NE) or nuclear pellet (NP) fractions; distinct sets of polypeptides bind unmodified vs. TFIIH-phosphorylated or P-TEFb-phosphorylated CTD. (A) Purification scheme for human TFIIH. (B) Example of a silver-stained gel showing immobilized GST only, GST-CTD, or TFIIH-phosphorylated CTD (GST-CTD-P) before (–) and after NE or NP incubation. Note that phosphorylated CTD state is maintained in GST-CTD-P samples. All samples had phosphatase inhibitors added. (C) Representative silver-stained gels showing proteins bound to GST only, unmodified GST-CTD, or TFIIH-phosphorylated CTD (GST-CTD-P), for both NE or NP binding experiments. (D) Purification scheme for human P-TEFb. (E) Example of a silver-stained gel showing immobilized GST only, GST-CTD, or P-TEFb-phosphorylated CTD (GST-CTD-P) before (–) and after NE or NP incubation. Note that phosphorylated CTD state is maintained in GST-CTD-P samples. All samples had phosphatase inhibitors added. (F) Representative silver-stained gels showing proteins bound to GST only, unmodified GST-CTD, or P-TEFb-phosphorylated CTD (GST-CTD-P), for both NE or NP binding experiments.

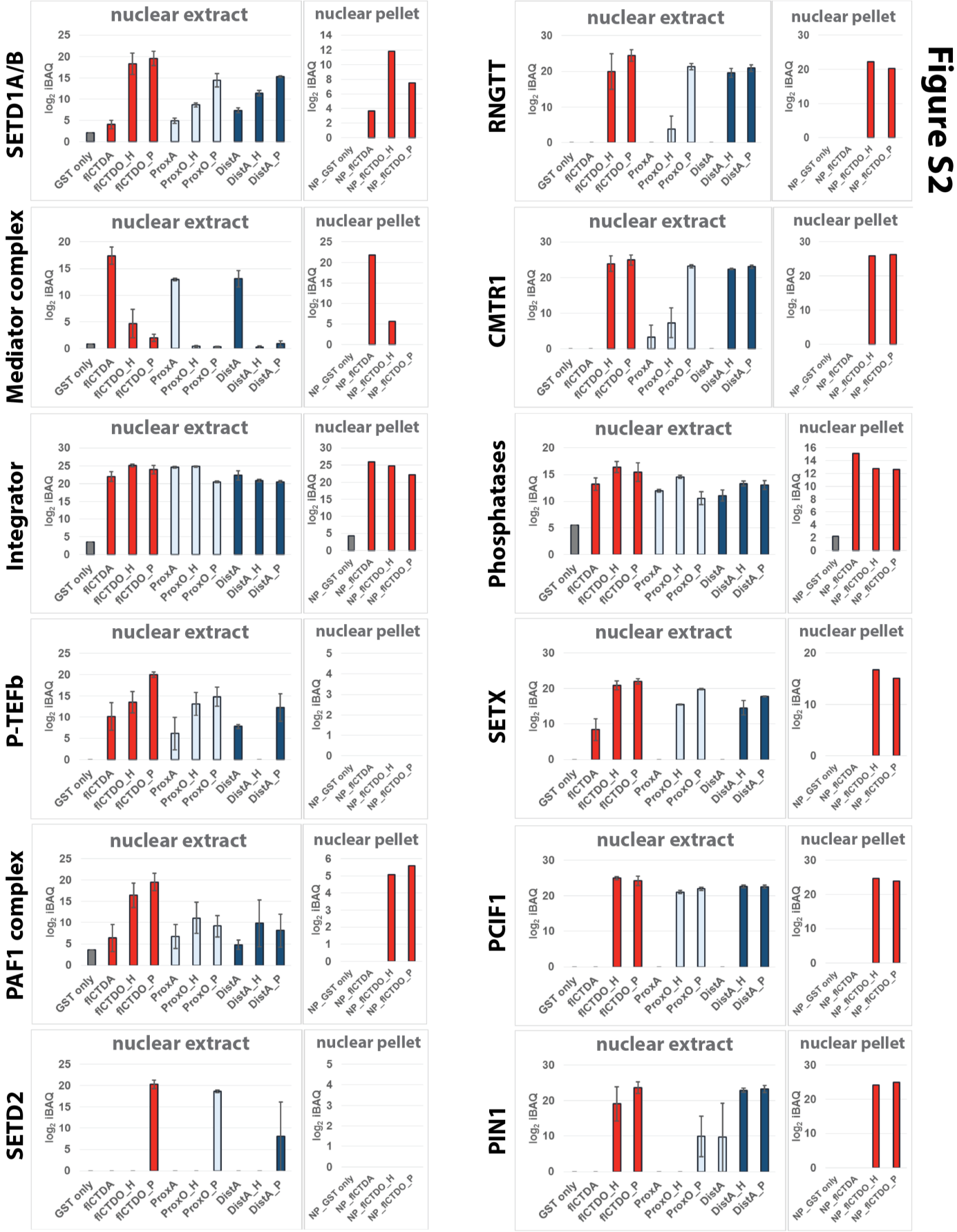

Figure S2 (related to Figure 2, 6). Summary of MS data for different proteins and protein complexes that bind unmodified or phosphorylated pol II CTD. Intensity-based absolute quantification (iBAQ) (Schwanhausser et al., 2011) data are shown plotted along the y-axis for select proteins or protein complexes indicated to the left of each plot. Data from experiments with nuclear extract or nuclear pellet are shown. For multi-subunit complexes (e.g. PAF1, Mediator), all subunits were combined. flCTDA = unmodified CTD, full-length; flCTDO_H = full-length CTD, TFIIH-phosphorylated; flCTDO_P = full-length CTD, P-TEFb-phosphorylated; ProxA = Proximal CTD (repeats 1-24), unmodified; ProxO_H = Proximal CTD, TFIIH-phosphorylated; ProxO_P = Proximal CTD, P-TEFb-phosphorylated; DistA = Distal CTD (repeats 25-52), unmodified; DistA_H = Distal CTD, TFIIH-phosphorylated; DistA_P = Distal CTD, P-TEFb-phosphorylated.

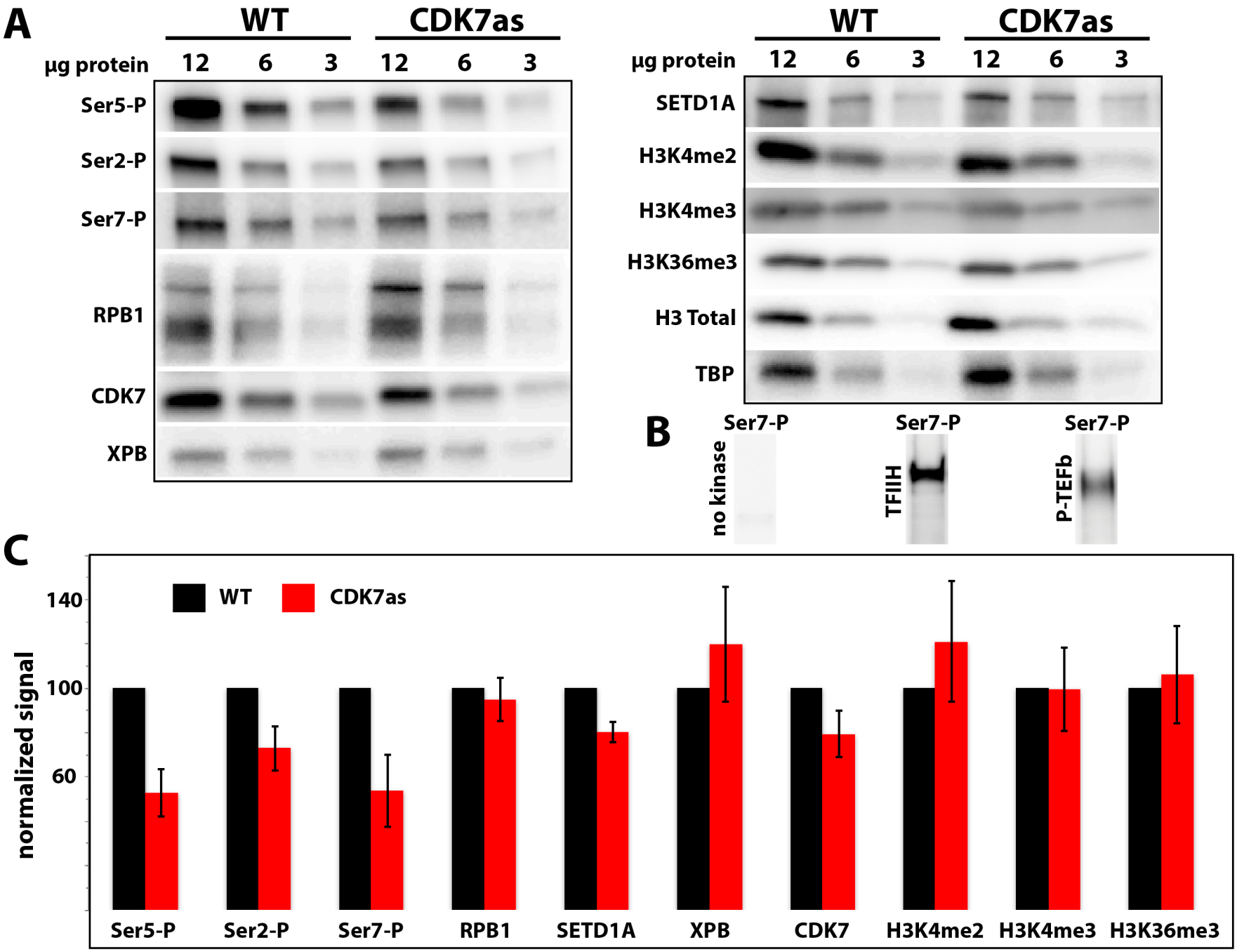

Figure S3 (related to Figure 3, 4, 5, 7). Comparison of protein levels and modifications in WT vs. CDK7as HCT116 cells, each treated with NM-PP1. (A) Representative western blots for the proteins or protein modifications shown at left; titration of total protein load is indicated at the top. (B) Both TFIIH and P-TEFb are Ser7 CTD kinases. Representative anti-Ser7-phospho western blots from in vitro kinase assays with the full-length pol II CTD. Each lane contained 12 µg GST-CTD after incubation with the kinase indicated. (C) Quantitation of western blot data from 3 technical replicates (± s.e.m.), which shows relative levels of proteins or protein modification states in WT vs. CDK7as cells. Western signal was normalized to RPB1 (for Ser5-P, Ser2-P, Ser-7-P), TBP, or total histone H3 (for histone modifications).

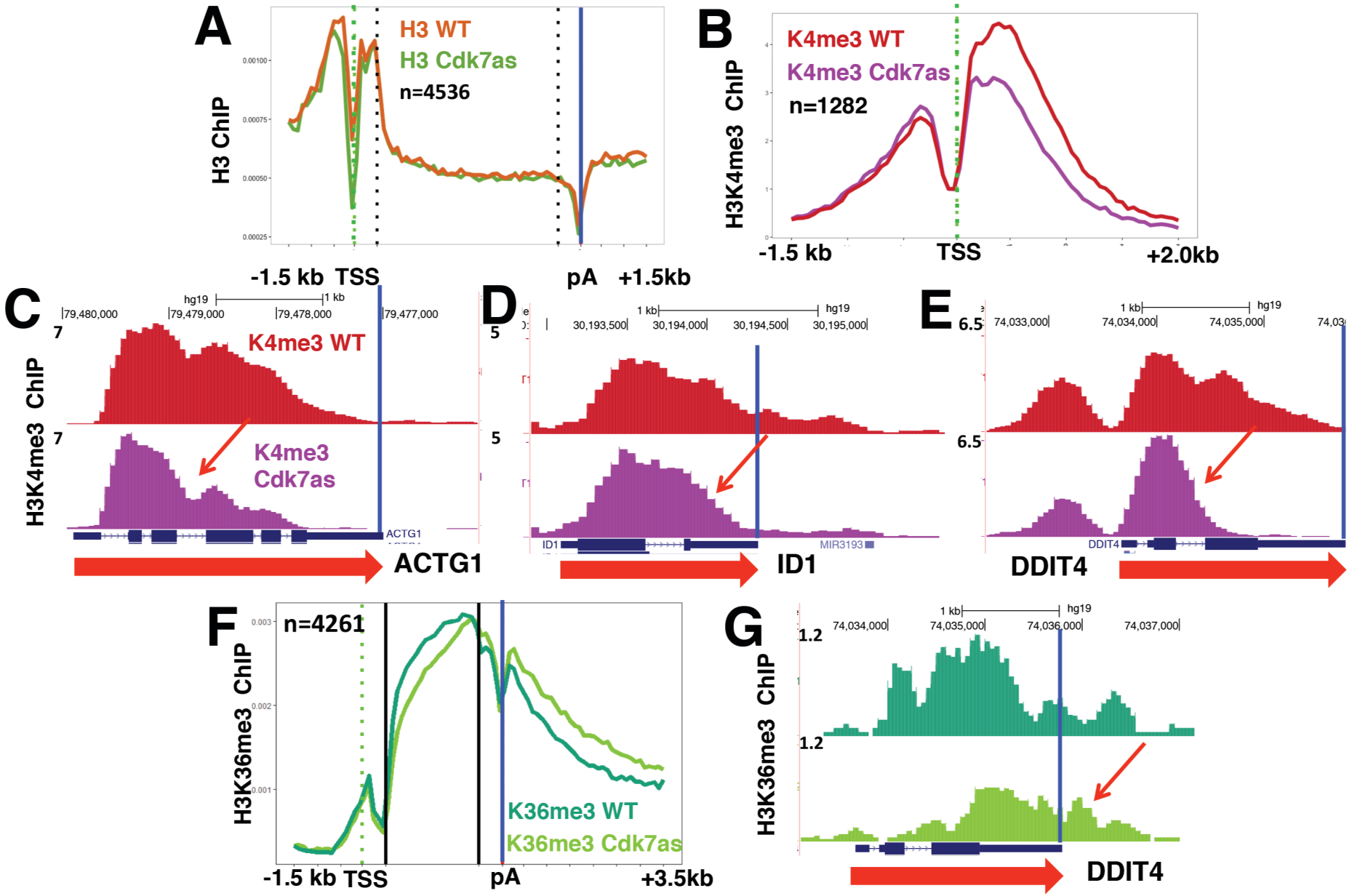

Figure S4 (related to Figure 4, 5, 7). CDK7 inhibition alters H3K4me3 and H3K4me3 distributions. (A) Metaplots of mean anti-H3 ChIP-Seq signals for well-expressed genes in WT and CDK7as cells, each treated with NM-PP1. Note the more prominent nucleosome free region at the TSS in CDK7as cells. (B) Metaplots of mean anti-H3K4me3 ChIP-Seq signals (normalized to the TSS) in WT and CDK7as cells, each treated with NM-PP1 (10μM, 24h) for a subset of genes with strongly reduced H3K4me3 signals upon CDK7 inhibition (Table S3). These data represent a biological replicate of data shown in Figure 4A. (C-E) UCSC genome browser screen shots of anti-H3K4me3 ChIP-Seq signals as in B. Note that CDK7 inhibition limits the spread of H3K4me3 into gene bodies (red arrows). These data represent a biological replicate of data shown in Figure 4B-D. (F) Metaplots of mean anti-H3K36me3 ChIP-Seq signals in WT and CDK7as cells, each treated with NM-PP1 inhibitor. (G) UCSC genome browser screen shots of anti-H3K36me3 ChIP-Seq signals in WT and CDK7as cells, each treated with NM-PP1 inhibitor. Note that CDK7 inhibition shifts the distribution of H3K36me3 toward 3' ends. The results in F, G are normalized to a mouse spike-in and represent a biological replicate of data shown in Figure 7D, F.

Figure S5

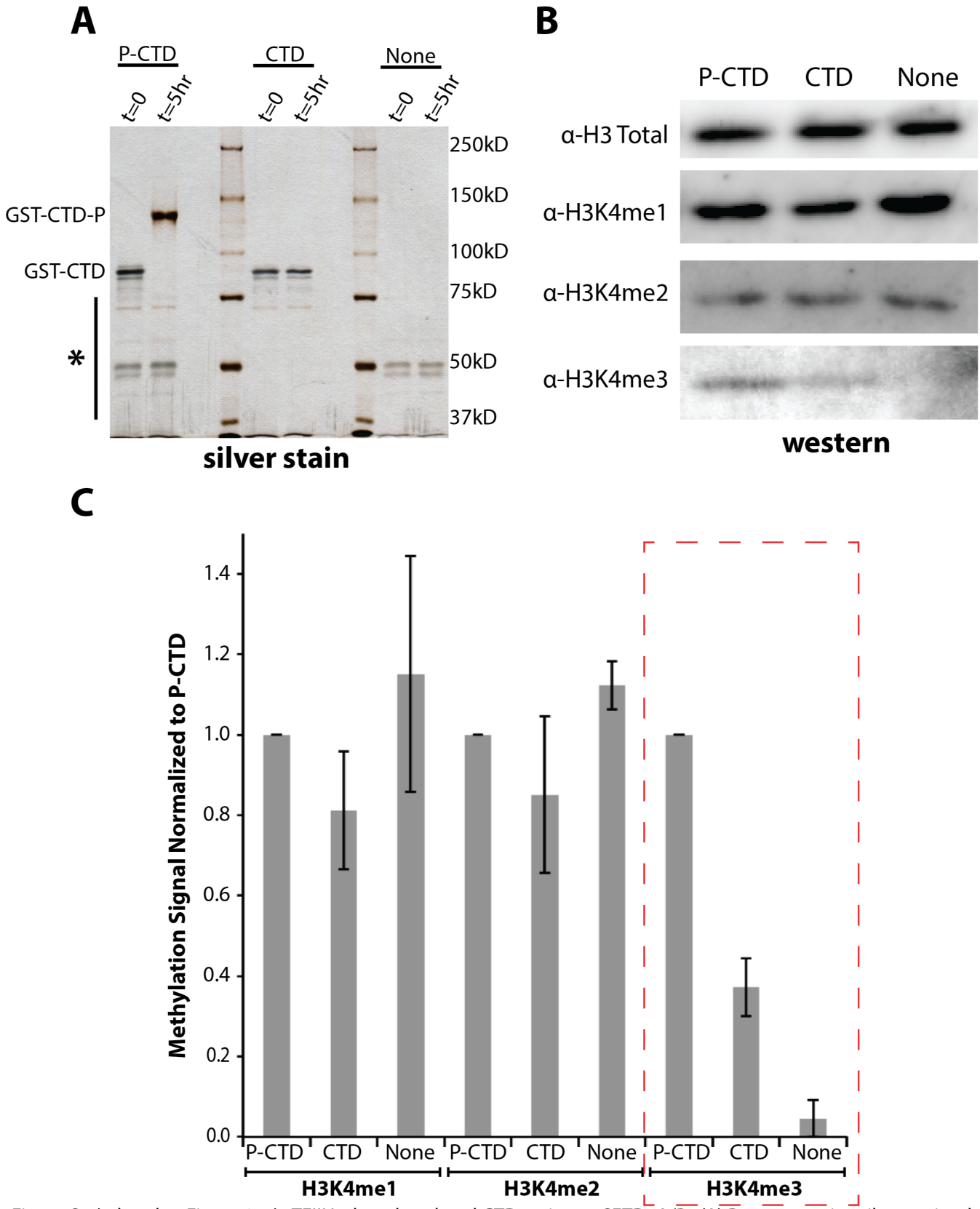

Figure S5 (related to Figure 2, 4). TFIIH-phosphorylated CTD activates SETD1A/B. (A) Representative silver-stained gel showing TFIIH-phosphorylated CTD (P-CTD), unmodified CTD (CTD), and no CTD (none); the "P-CTD" and "None" samples each contained TFIIH, but only the P-CTD sample included ATP to achieve a fully phosphorylated CTD, as shown. These fractions were added to methyltransferase assays with SETD1A or SETD1B in the presence of nucleosomal templates (see Methods). Asterisk: bands corresponding to TFIIH and eluted antibody used to purify TFIIH. (B) Representative western blot data following incubation of SETD1B with nucleosomes, SAM, and the corresponding CTD supplement indicated at the top. (C) Relative quantitation (± s.e.m.; for H3K4me1, H3K4me2, and H3K4me3, n = 3, 2, 3 replicate experiments, respectively) of H3K4 methyl marks following incubation of SETD1B with the pol II CTD fraction indicated (None = buffer + TFIIH only). Data for H3K4me1, H3K4me2, or H3K4me3 were normalized to signal from P-CTD samples, which was set to 1. Note that the phosphorylated CTD specifically affected levels of tri-methylated H3K4 with SETD1B, not mono- or di-methyl (red box). Similar data were obtained for SETD1A complexes.

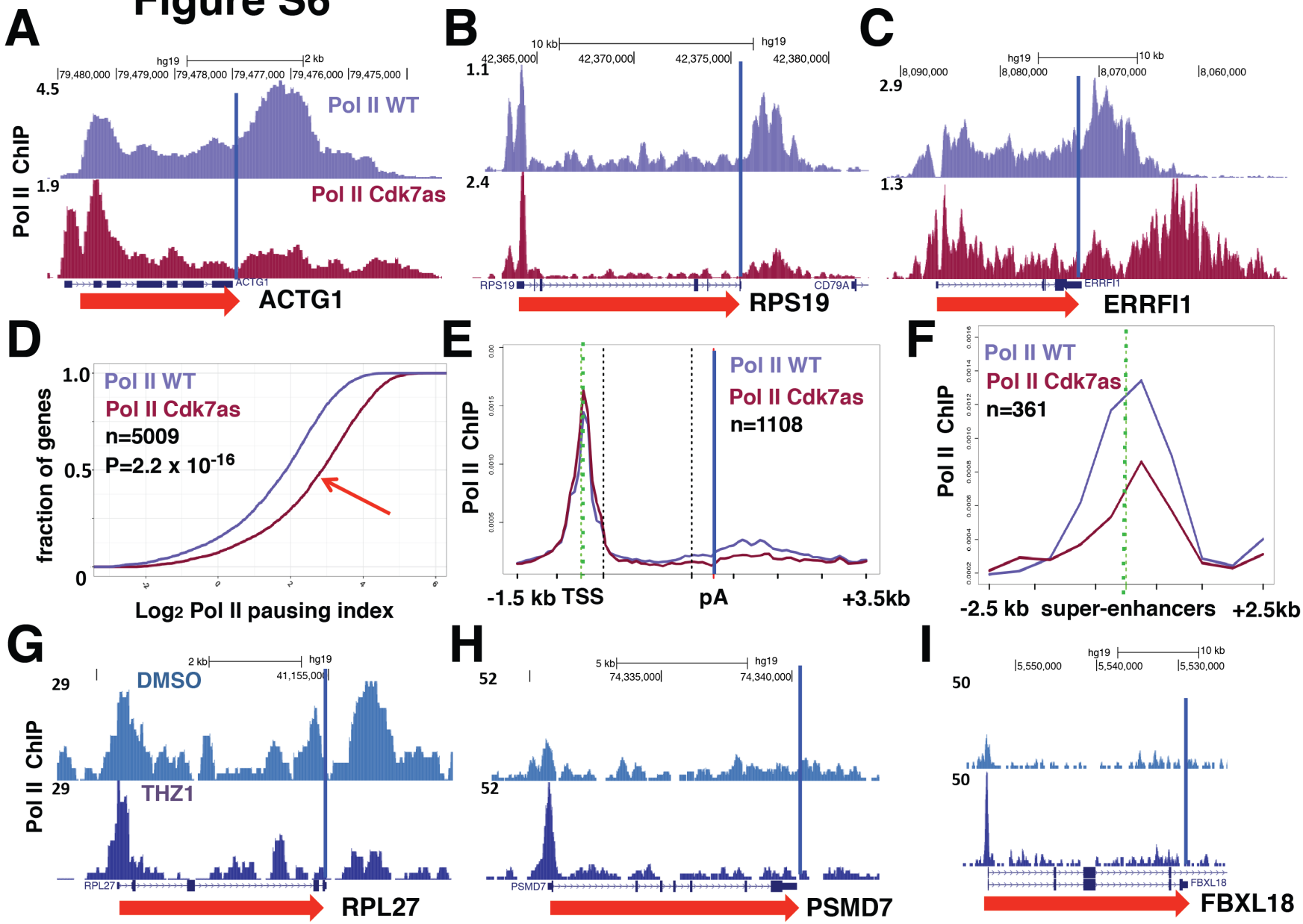

Figure S6 (related to Figure 5). Pol II pausing index and super-enhancer occupancy are altered upon inhibition of CDK7 activity. (A-C) UCSC genome browser screenshots of anti-pol II ChIP-Seq signals in WT and CDK7as HCT116 cells, each treated with NM-PP1 inhibitor (10μM, 24h). Note CDK7 inhibition causes a 5'-shift of pol II density and extends pol II occupancy in 3' flanking regions. (D) CDK7 inhibition increases pol II pausing index. Cumulative index plots of pausing index (log2 pol II promoter density/pol II gene body density; promoter defined as -30 to +300 bases relative to TSS and gene body as +301 to poly(A) site), calculated from anti-pol II ChIP signals in WT and CDK7as cells, each treated with NM-PP1. Note rightward shift of the curve in CDK7as cells (red arrow). P-value calculated by two-sided Kolmogorov-Smirnov test. Data in panels A-D are biological replicates of experiment shown in Figure 5A-C, E. (E) Pol II ChIP-Seq at genes that showed reduced H3K4me3 levels. (F) CDK7 inhibition reduces pol II occupancy at super-enhancers. Metaplots of mean anti-pol II ChIP-Seq signals in WT and CDK7as cells, each treated with NM-PP1 inhibitor, from the dataset in Figure 5A-E. Super-enhancers are as defined in (Loven et al., 2013). (G-I) UCSC genome browser screenshots of anti-pol II ChIP-Seq signals in HCT116 cells treated with THZ1 (1 hr, 1 μM) or DMSO control as in Figure 5F, G. Note that THZ1 shifts pol II density toward gene 5'-ends.

Figure S7

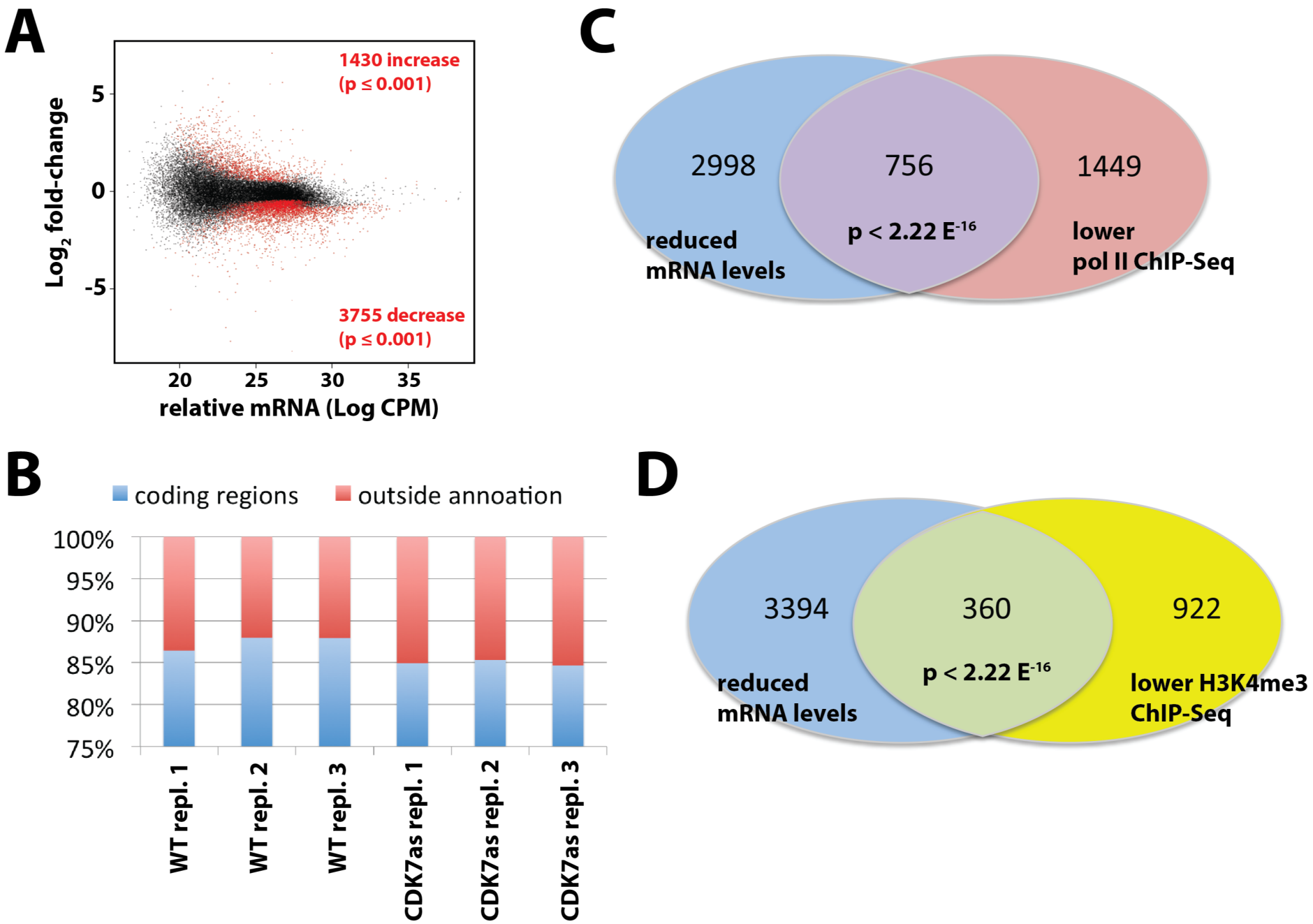

Figure S7 (related to Figure 4, 5). Gene expression changes (RNA-Seq) in WT vs. CDK7as HCT116 cells. (A) MA plot comparing average mRNA level and the log2-fold change between WT and CDK7as cells treated with NM-PP1 inhibitor. (B) Based upon RNA-Seq data, the percentage of tags in annotated regions and outside of annotated regions was calculated for each of the biological replicate samples shown. (C) Venn diagram showing the overlap of genes down-regulated by RNA-Seq with those that showed reduced pol II occupancy in the gene body by ChIP-Seq. The p-value was calculated by hypergeometric test. (D) Venn diagram showing overlap among genes with reduced mRNA levels (based upon RNA-Seq data) and reduced H3K4me3 levels (based upon ChIP-Seq data).

Table S2A: Proteins binding unmodified CTD, not TFIIH-phosphorylated CTD

CA9	KRT6B	MED16	MED29
CAPZA	LIMCH1	MED17	MED30
CAPZB	LMO7	MED18	MED31
CTNND1	MED1	MED19	MYO1C
DSP	MED4	MED20	MYO1G
ELL	MED6	MED21	PICALM
GNAI1	MED7	MED22	SPTBN2
GNAI2	MED8	MED23	STOM
GNB1	MED9	MED24	TOX4
GNB2	MED10	MED25	WWP1
ITCH	MED11	MED26	WWP2
ITGA5	MED14	MED27	ZNF655
KPNA6	MED15	MED28	

Table S2B: Proteins binding TFIIH-phosphorylated CTD, not unmodified CTD

ACTN1	DDX5	IQGAP1	RPS7
ACTN4	DHX15	MARS	RPS8
ACTR2	DPY30	MTR1	RPSA
ALDH18A1	ECH1	MYO1E	SCAF4
ASH2L	ENSG00000250151	NOLC1	SEPT.8
BOD1L1	ERCC3	PCIF1	SETD1A
CAPRIN1	FASN	PIN1	SETD1B
CDC73	FLOT1	POLR2B	SETX
CHD4	FOLR1	POLR2C	SKIV2L2
CMTR1	GLUD1	PPP1CB	TRIM25
CORO1C	HCFC1	PSMD2	TUBA8
CSTF2	HNRNPC	PSME2	WDR82
CTR9	HNRNPH1	RBBP5	YBX1
CXXC1	HNRNPH2	RHOA	ZC3H4
	HNRNPL	RNGTT	

Table S2. (**A**) List of proteins that differentially bind unmodified CTD vs. TFIIH-phosphorylated CTD. (**B**) List of proteins that differentially bind TFIIH-phosphorylated CTD vs. unmodified CTD. Related to **Figure 2**.

Table S6: Proteins binding P-TEFb-phosphorylated but not TFIIH-phosphorylated CTD

C22orf28	HIST1H4H	RAD50	SF3A1
CDC5L	HNRNPR	RBM25	SMARCC2
CHERP	ILF2	RECQL5	SMC4
CPSF1	ILF3	RIF1	SRRT
CPSF3	KIAA1967	SCAF1	TBL1XR1
DARS	PHF3	SCAF11	TOX4
DDX21	PHRF1	SCAF8	U2SURP
ELL	PRPF40A	SCAI	ZNF207
GATAD2B	RAD21	SETD2	

Table S6. List of proteins that differentially bind P-TEFb-phosphorylated CTD vs. TFIIH-phosphorylated CTD. Related to **Figure 6**.